PHYSICAL REVIEW B **66**, 094420 (2002)

Frustration-driven structural distortion in $VOMoO_4$

P. Carretta,* N. Papinutto, C. B. Azzoni, M. C. Mozzati, and E. Pavarini
Dipartimento di Fisica "A. Volta" e Unitá INFM di Pavia, Via Bassi 6, 27100 Pavia, Italy

S. Gonthier and P. Millet
Centre d'Elaboration des Matériaux et d'Etudes Structurales, CNRS, 31055 Toulouse Cedex, France

(Received 23 April 2002; published 17 September 2002)

Nuclear magnetic resonance (NMR), electron paramagnetic resonance (EPR), magnetization measurements, and electronic structure calculations in $VOMoO_4$ are presented. It is found that $VOMoO_4$ is a frustrated two-dimensional antiferromagnet on a square lattice with competing exchange interactions along the side (J_1) and the diagonal (J_2) of the square. From magnetization measurements J_1+J_2 is estimated around 155 K, in satisfactory agreement with the values derived from electronic structure calculations. Around 100 K a structural distortion, possibly driven by the frustration, is evidenced. This distortion induces significant modifications in the NMR and EPR spectra which are possibly due to valence fluctuations. The analysis of the spectra suggests that the size of the domains where the lattice is distorted progressively grows on cooling as the temperature approaches the transition to the magnetic ground state at $T_c \simeq 42$ K.

DOI: 10.1103/PhysRevB.66.094420 PACS number(s): 76.60.Es, 76.75.+i, 75.10.Jm

I. INTRODUCTION

In the last decade transition metal oxides have attracted a lot of interest in view of the rich phenomenology induced by the strong electronic correlations. The properties of these oxides are rather peculiar once the interaction of the electrons with the lattice becomes relevant. This is the driving mechanism of several phenomena such as, for example, superconductivity, colossal magnetoresistivity,[1] and the spin-Peierls transition.[2] Recently, the importance of the coupling between the electron spin and lattice has emerged for a new class of materials, the frustrated antiferromagnets.[3] In this case, the magnetoelastic coupling tends to relieve the degeneracy of the ground state caused by the frustration of the magnetic exchange couplings.[4] This is the situation observed, for example, in Li_2VOSiO_4,[5,6] which is a frustrated two-dimensional $S=1/2$ antiferromagnet (2DFQHAF) on a square lattice with competing exchange interactions along the side (J_1) and diagonal (J_2) of the square. This compound has $J_1 \simeq J_2$ ($J_1+J_2 \simeq 8.5$ K) and represents a prototype of the two-dimensional J_1-J_2 model, which was extensively studied from a theoretical point of view in the last decade.[7] In the absence of any spin-lattice coupling the ground state is double degenerate, the two states corresponding to collinear phases (hereafter called I and II) which differ in the orientation of the magnetic wave vector.[8] The magnetoelastic coupling leads to a lattice distortion at $T_{dist} \simeq (J_1+J_2)/2$, which affects ^{29}Si and ^{7}Li NMR spectra,[5,6] and Li_2VOSiO_4 is observed to collapse always in one of the two possible ground states.

Another 2DFQHAF, nearly isostructural to Li_2VOSiO_4,[9] is $VOMoO_4$.[10] The structure of these compounds is formed by pyling up layers of $SiVO_5$ for the former and of $MoVO_5$ for the latter. These layers contain VO_5 pyramids separated by $(Si,Mo)O_4$ tetrahedra (see Fig. 1). The only difference is that in Li_2VOSiO_4 a plane of Li^+ ions is present between the $SiVO_5$ layers. $VOMoO_4$ has been recently investigated by Shiozaki and co-workers,[11] which, however, have considered it as a protoype of a weakly one-dimensional antiferromagnet[12] instead of a 2DFQHAF, as will be shown in the following. The interest in $VOMoO_4$ stems from the fact that although the structure is very similar to the one of Li_2VOSiO_4, the exchange couplings are more than an order of magnitude larger. Thus the comparison of the properties of the two systems would allow us to understand if frustration is indeed the driving mechanism for the observed structural distortions.

In this paper nuclear magnetic resonance (NMR), electron paramagnetic resonance (EPR), and magnetization measurements in $VOMoO_4$ powders are presented. The temperature dependence of the susceptibility evidences that also, for $VOMoO_4$, $J_1 \simeq J_2$. At temperatures below J_1+J_2—namely, at $T_{dist} \simeq 0.64(J_1+J_2)$—$VOMoO_4$ shows a lattice distortion possibly driven by the magnetic frustration. The distortion seems to induce valence fluctuations, not observed in

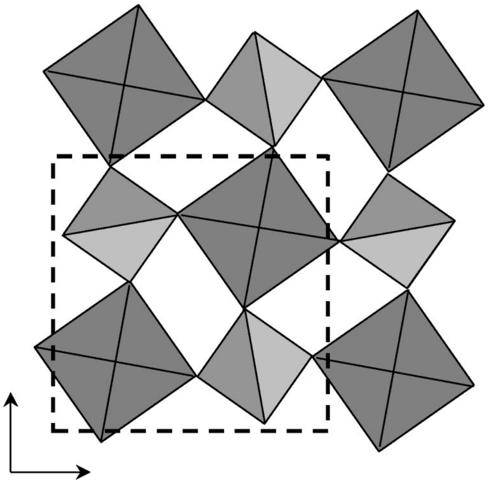

FIG. 1. Structure of $VOMoO_4$ projected along [001]. VO_5 pyramids (black) run parallel to the line of sight and are connected by MoO_4 tetrahedra (gray). For details see Ref. 10. The dashed line shows the projection of the unit cell with $a=6.6078$ Å.

Li_2VOSiO_4, with a charge transfer from V^{4+} to Mo^{6+}. Moreover, it is found that domains of distorted lattice, with a size which progressively grows on cooling, are formed below T_{dist}. The magnitude of the superexchange couplings was estimated from electronic structure calculations and the two-dimensional character of $VOMoO_4$ evidenced. Finally, the role of Mo *d* orbitals in determining the differences with respect to Li_2VOSiO_4 is emphasized.

The paper is organized as follows: in Sec. II the technical aspects and the experimental results will be shown, while in Sec. III analysis of the data, including the electronic structure calculation, and analysis of NMR relaxation rates and of the lattice distortion will be presented. The final conclusions are summarized in Sec. IV.

II. EXPERIMENTAL ASPECTS AND EXPERIMENTAL RESULTS

A. Sample preparation, EPR, and magnetization measurements

$VOMoO_4$ powders were obtained by solid-state reaction starting from a stoichiometric mixture of MoO_3 (Aldrich, 99.5+%), V_2O_5 (Aldrich, 99.99%), and V_2O_3 heated in a vacuum-sealed quartz tube at 675 °C for 24 h. V_2O_3 itself was prepared by reducing V_2O_5 (Aldrich, 99.6+%) under hydrogen at 800 °C. The sample purity was analyzed by means of x-ray powder diffraction and all diffraction peaks corresponded to the ones of $VOMoO_4$ (JCPDS file: 18-1454). Single crystals were prepared by chemical transport reaction starting from a stoichiometric mixture of the starting materials and TeCl4 (10% in weight). The mixture was sealed under vacuum and heated for 24 h at 575 °C, then slowly cooled at 10 C/h down to room temperature.

EPR spectra were recorded with an *X*-band spectrometer equipped with a standard microwave cavity and a variable-temperature device. The measurements were performed both on powders and on a single crystal of volume $V \leqslant 0.03\ \mathrm{mm}^3$. The EPR powder spectra are characterized by a line shape which becomes progressively more asymmetric as the temperature is lowered below 130 K [see Fig. 2(a) and the inset to Fig. 3(a)]. These spectra can be quite well simulated by considering a temperature-independent cylindrical $\tilde{g}$ tensor with components $g_c = 1.960$ and $g_{ab} = 1.932$. These values are consistent with the estimates of V^{4+} $\tilde{g}$ in the framework of the crystal field approximation, by assuming a spin-orbit coupling $\lambda = 150\ \mathrm{cm}^{-1}$ and some covalency between V and O.[13] It should be noticed that g_c and g_{ab} values are reversed with respect to what one might expect just by looking at the spectrum at $T = 70$ K in Fig. 3(a). In fact, one would be tempted to associate the low-field most intense peak with V^{4+} in grains where $\vec{H} \perp \vec{c}$, while the less intense one with those grains with $\vec{H} \| \vec{c}$. However, if this assignment is made the data cannot be fitted adequately. The increase in the intensity of the low-field peak with respect to the high-field one, below 130 K (see the inset to Fig. 3), has rather to be associated with a faster decrease of the linewidth ΔH for $\vec{H} \| \vec{c}$ than for $\vec{H} \perp \vec{c}$ (see Fig. 3). These results can be suitably compared to the ones derived from EPR measurements on a single crystal. The crystal was mounted on a sample holder that allowed one to rotate the field in the *ac* plane. V^{4+} EPR spectra on the crystal confirmed that the $\tilde{g}$ tensor is practically temperature independent down to $T_c \simeq 42$ K with g_c and g_{ab} identical to the ones derived from the EPR powder spectra. Moreover, the temperature dependence of ΔH is the same found for the powders, characterized first by a decrease on cooling, then a minimum around 60 K, and finally an increase as the temperature approaches T_c (see Fig. 3). The temperature dependence of the area of the EPR powder spectra, which in principle is proportional to the static uniform susceptibility χ, is shown in Fig. 4. Above 100 K the temperature dependence is very similar to the one derived for χ

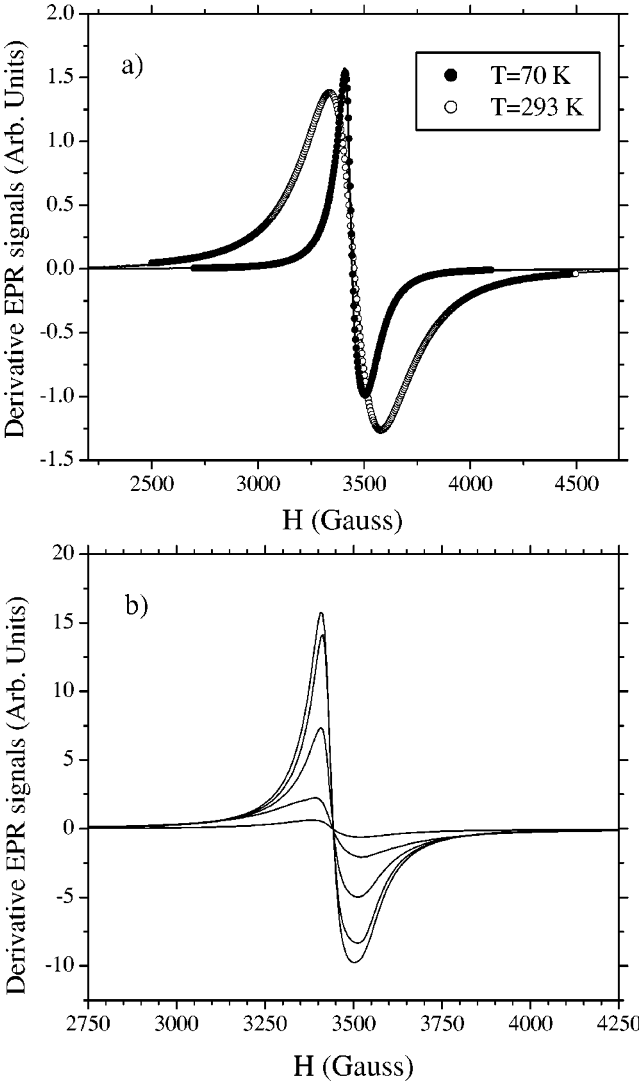

FIG. 2. (a) Derivative of the EPR powder spectra (solid lines) at $T = 293$ and 70 K. The circles show the best fit of the two spectra, used to determine *g* and ΔH. Notice that, in order to better illustrate the different asymmetry, the intensity of two spectra was not normalized. (b) Derivative of the EPR powder spectra for five selected temperatures between 69 K and T_c. The temperatures, moving from the most intense to the less intense signal, are $T = 69$, 59, 49, 45.5, and 42 K. A marked decrease in the intensity of the EPR signal on cooling is evident.

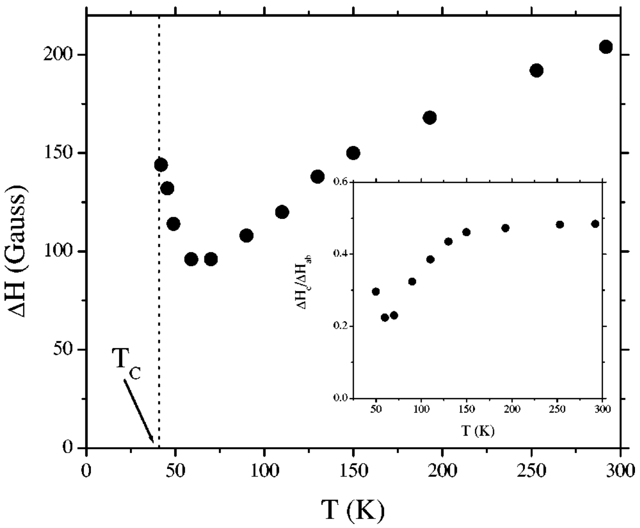

FIG. 3. Temperature dependence of the peak to peak width of the EPR powder spectrum in $VOMoO_4$. In the inset the ratio between the EPR linewidth for $\vec{H}\|$ and $\perp\vec{c}$, estimated from the analysis of the powder spectra, is reported.

from magnetization measurements (see paragraph below); however, below this temperature a rapid decrease of the EPR intensity is evident [see Fig. 2(b)], down to T_c. Then, below T_c a small signal with a different $\tilde{g}$, possibly arising from impurities, starts to be detected.

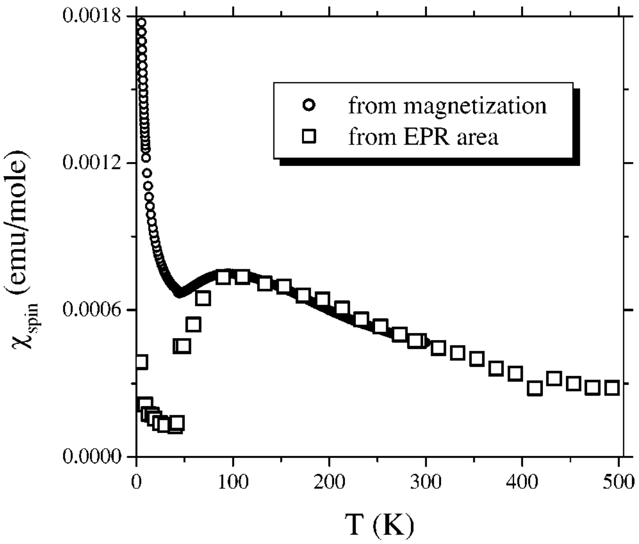

FIG. 4. Temperature dependence of the area of the EPR signal (squares) and of the spin susceptibility (circles) measured experimentally with a SQUID magnetometer after subtraction of the Van Vleck contribution (see text). The area of the EPR signal, which in principle is proportional to the spin susceptibility, was rescaled to match the value of the spin susceptibility at room temperature.

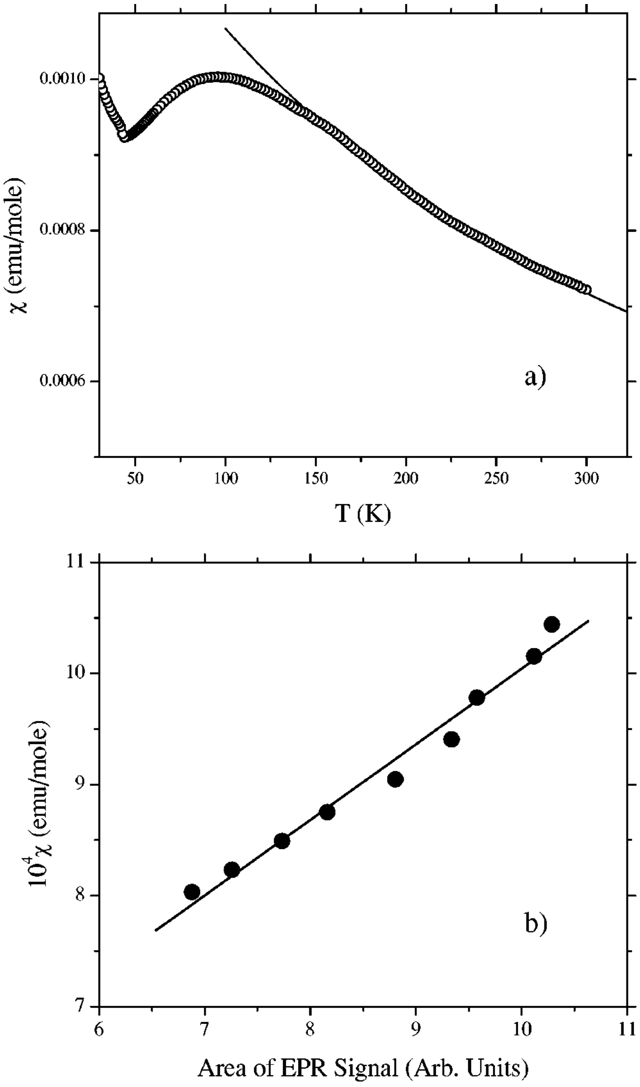

FIG. 5. (a) Temperature dependence of the susceptibility in $VOMoO_4$, for $H = 1$ kG. The solid line shows the high-temperature Curie-Weiss behavior for $\Theta = 155$ K. (b) Plot of the susceptibility measured with the SQUID magnetometer (after subtraction of the atomic diamagnetic contribution) vs the area of the EPR signal, with the temperature as an implicit parameter. The intercept of the solid line was used to derive Van Vleck susceptibility.

Magnetization (M) measurements were performed on $VOMoO_4$ powders using a commercial Quantum Design MPMS-XL7 superconducting quantum interenference device (SQUID) magnetometer. The temperature dependence of the susceptibility, defined as $\chi = M/H$ with H the intensity of the applied magnetic field, is shown in Fig. 5(a). One observes a high-temperature Curie-Weiss behavior, a broad maximum around 100 K typical of low-dimensional antiferromagnets, and a kink at $T_c \simeq 42$ K, which indicates the presence of a phase transition. This trend is the same already observed by Shiozaki *et al.*[11] At temperatures well above the maximum the susceptibility is given by

$$\chi(T) = \frac{C}{T + \Theta} + \chi_{VV}, \tag{1}$$

where C is the Curie constant, Θ the Curie-Weiss temperature, and χ_{VV} Van Vleck susceptibility. In order to estimate Θ, which for a 2DFQHAF on a square lattice is equal to $J_1 + J_2$, one has to determine first the value of χ_{VV}. Since

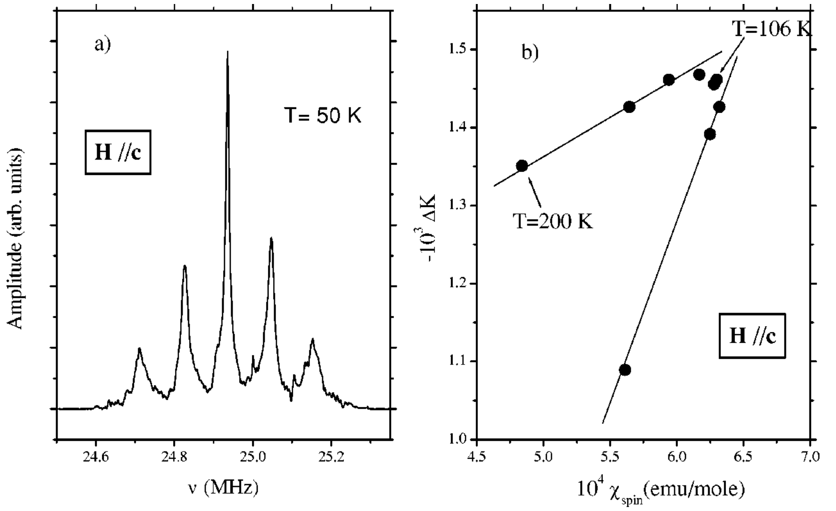

FIG. 6. (a) ^{95}Mo NMR powder spectra in VOMoO$_4$ oriented powders for $H=9$ T along the *c* axis. (b) ^{95}Mo NMR shift in VOMoO$_4$ for $\vec{H}\parallel c$ vs the spin susceptibility, measured with the SQUID magnetometer, after subtraction of the Van Vleck term. The temperature, which is an implicit parameter, is shown for a few selected points. The solid lines evidence the change of slope, i.e., of hyperfine coupling, on cooling.

χ_{VV} does not contribute to the EPR signal, its value can be directly determined by plotting χ measured with the SQUID against the EPR area for $T>150$ K [see Fig. 5(b)]. One finds $\chi_{VV}=3.5\times10^{-4}$ emu/mol, a value consistent with the separation between the t_{2g} levels derived from crystal field calculations and close to the one estimated for Li$_2$VOSiO$_4$, where V^{4+} has practically the same coordination. Then, by fitting the susceptibility data for $T>150$ K, with Eq. (1) one derives $\Theta=155\pm20$ K.

B. NMR spectra and relaxation rates

^{95}Mo NMR spectra were recorded both on unoriented as well as on magnetically aligned powders by summing the Fourier transform of half of the echo signal recorded at different frequencies. The powders were oriented in epoxy resin with the magnetic field direction along the *c* axis which, as can be seen from a close inspection of the crystal symmetries, corresponds to the principal axis of the electric field gradient (EFG) at ^{95}Mo nuclei. The NMR spectra in the oriented powders are characterized by five well-defined peaks [see Fig. 6(a)] separated by $\nu_Q\simeq106$ kHz. For a cylindrical EFG tensor, as the one of ^{95}Mo in VOMoO$_4$, one has that[14] $\nu_Q=3eV_{zz}Q(1-\gamma_\infty)/20h$, where V_{zz} is the principal component of the EFG tensor, $Q=-0.019$ barn the ^{95}Mo electric quadrupole moment, and $(1-\gamma_\infty)$ the Sternheimer antishielding factor. One can compare the experimental value of ν_Q with the one derived from an estimate of the EFG based on lattice sums, within a point charge approximation and taking $(1-\gamma_\infty)\simeq24.861$, as estimated theoretically.[15] One obtains $\nu_Q\simeq102.5$ kHz, in remarkable agreement with the experimental finding. On the other hand, the powder spectra are characterized by a sharp central peak, corresponding to the $1/2\rightarrow-1/2$ transition, and by an underlying broad powder spectrum. Below T_c the ^{95}Mo NMR powder spectrum broadens, as expected in the presence of a magnetic order, yielding a local field at the nuclei which is randomly oriented with respect to the external field.

It is interesting to analyze the temperature dependence of the shift of the central line in the oriented powders for $\vec{H}\parallel c$ and for the unoriented powders, which probe mainly the shift for $\vec{H}\perp c$. As reported in Fig. 7(a) one observes that the resonance frequency of the peak in the unoriented powders has a temperature dependence which is exactly the opposite of the one observed for the susceptibility (see Fig. 5). Since the quadrupolar corrections to the central line shift are negligible, one can assert that the opposite behavior of these two quantities is due to a negative hyperfine coupling constant (*A*) between the ^{95}Mo nucleus and the four nearest-neighbor V^{4+} ions. In fact, the shift of the NMR line can be written as

$$\Delta K=\frac{4A\chi}{g\mu_B N_A}+\delta, \tag{2}$$

with μ_B the Bohr magneton and δ the chemical shift. Hence, by plotting ΔK vs χ [see Fig. 7(b)] one can derive the hyperfine coupling constant *A* which for $T\leqslant100$ K turns out $A_{pow}\simeq-9$ kOe. In Fig. 7(b) one clearly observes that around 100 K there is a sizable change of slope which has to be associated with a marked decrease in the hyperfine coupling and suggests that around 100 K significant modifications in the local structure around Mo^{6+} are taking place. Above 110 K one has $A_{pow}\simeq-2.5$ kOe. The shift measurements in the oriented powders yield quantitatively similar results [see Fig. 6(b)], pointing out that the hyperfine coupling is quite isotropic. The values for the component of the hyperfine coupling tensor for $\vec{H}\parallel c$ turn out to be $A_c\simeq-11.5$ kOe for $T<100$ K and $A_c\simeq-2.7$ kOe for $T>110$ K. Finally, it must be mentioned that while above 100 K the width of the central line is temperature independent, a sizable broadening is observed below 100 K, the linewidth for $\vec{H}\parallel c$ increasing from about 2.3 kHz at 106 K to about 6.5 kHz at 50 K. This fact suggests an increasing inhomogeneity at the microscopic level.

Nuclear spin-lattice relaxation rate $1/T_1$ was measured on the central ^{95}Mo NMR line by means of a saturation recovery pulse sequence. The length of the saturation sequence was much shorter than T_1 while the repetition time was much longer than the spin-lattice relaxation time to allow nuclear spins to reach thermal equilibrium between each scan. The recovery law was found to be multiexponential, as

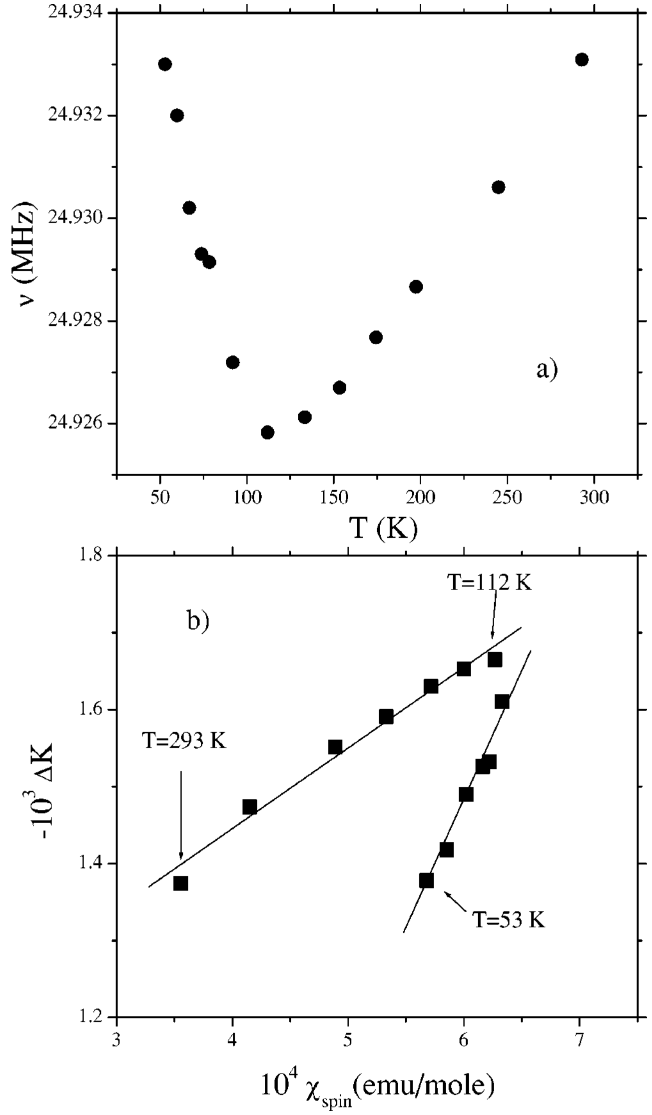

FIG. 7. (a) Temperature dependence of the resonance frequency for ^{95}Mo NMR central line. (b) ^{95}Mo NMR shift of the central line in VOMoO$_4$ unoriented powders plotted against the spin susceptibility, measured with the SQUID magnetometer, after subtraction of the Van Vleck term. The temperature, which is an implicit parameter, is shown for a few selected points. The solid lines evidence the change of slope, i.e., of hyperfine coupling, on cooling.

expected. Now, the point is whether the relaxation process is driven by fluctuations of the hyperfine field or of the EFG. As we shall see later on in the discussion of the experimental results, the magnetic relaxation mechanism is the dominant one (Sec. III B). Then, the recovery law for the nuclear magnetization $m_z(t)$ is

$$\frac{m_z(t\rightarrow\infty)-m_z(t)}{m_z(\infty)}=\frac{1}{35}e^{-t/T_1}+\frac{8}{45}e^{-6t/T_1}+\frac{50}{63}e^{-15t/T_1}. \tag{3}$$

The values of $1/T_1$ derived from the fit of the experimental data with Eq. (3) are reported in Fig. 8. One notices a decrease of the relaxation rate on cooling down to about 90 K, then a plateau and a peak at T_c, as expected for a second-order phase transition.

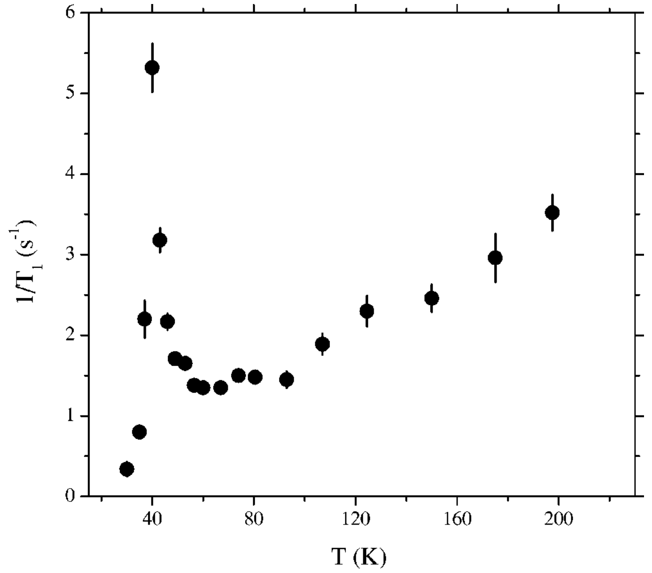

FIG. 8. Temperature dependence of ^{95}Mo NMR $1/T_1$ in VOMoO$_4$ for the central line in a magnetic field of 9 T, derived by fitting the recovery of nuclear magnetization with Eq. (3).

The decay of the echo signal after a $\pi/2$-τ-π pulse sequence was observed to be practically exponential. The decay of the amplitude of ^{95}Mo echo signal arises in principle from three different contributions: namely,

$$E(2\tau)=E(0)[D(2\tau)e^{-2\tau/T_1^R}e^{-\Delta\omega'^2\tau_c^2 f(2\tau,\tau_c)}]. \tag{4}$$

The first term $D(2\tau)$ is the decay associated with the ^{95}Mo nuclear dipole-dipole interaction. The second moment M_2 of the corresponding frequency distribution was determined on the basis of lattice sums taking into account the natural abundance of ^{95}Mo.[14] It was found that $\sqrt{M_2}=90\ \mathrm{s}^{-1}$. If one takes this value and assumes a Gaussian decay, sizable deviations from the exponential behavior should be detected, mainly at low temperature. The absence of any evidence for such a Gaussian deviation could stem from the low natural abundance of ^{95}Mo nuclei which leads, as for diluted nuclear spins, to a dipolar contribution to the echo decay which is neither Gaussian nor exponential.[14] Then one has to approximate the nuclear dipole contribution to the echo decay with a moment expansion. $D(2\tau)$ was expanded up to the fourth moment and its expression was used to fit the data up to $2\tau\simeq 1/(2\sqrt{M_2})$. It must be remarked that, in anyway, above 120 K the contribution of $D(2\tau)$ to the echo decay is small with respect to the one due to the third term in Eq. (4).

The second term in Eq. (4) is the Redfield contribution to the echo decay. When just the central transition of an $I=5/2$ nucleus is irradiated and in the case of an isotropic spin-lattice relaxation rate one has[17] $1/T_1^R=9/T_1$. The third term is the dominant one and originates from a low-frequency dynamics characterized by a correlation time τ_c which modulates the resonance frequency of the nuclei by $\Delta\omega'$. The observation that the echo decay is exponential

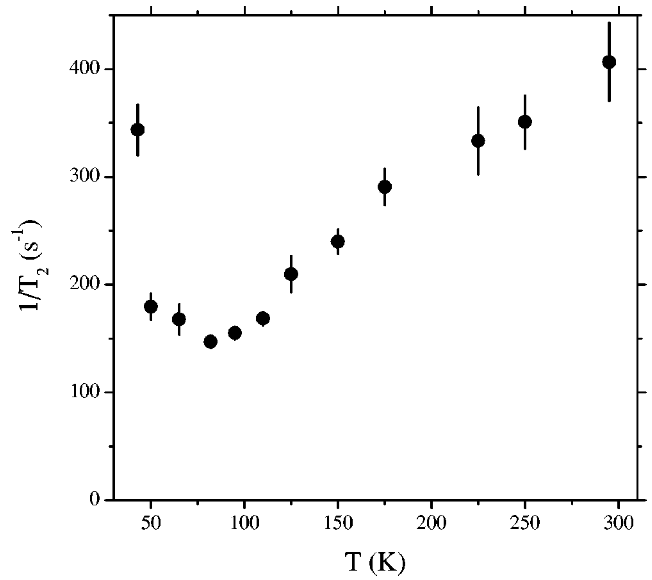

FIG. 9. Temperature dependence of $1/T_2$ in $VOMoO_4$ powders for $H=9$ T, derived by fitting the echo decay of ^{95}Mo central transition with Eq. (4).

implies that $\Delta\omega'\tau_c \ll 1$, so that $f=2\tau/\tau_c$ and the last term of Eq. (4) becomes $\exp(-2\tau/T_2)$, with[14] $1/T_2=\Delta\omega'^2\tau_c$. The temperature dependence of $1/T_2$ derived by fitting the echo decay with Eq. (4) is shown in Fig. 9.

Finally, it must be mentioned that a ^{51}V NMR signal was detected, with a temperature dependence of $1/T_1$ and of $1/T_2$ very similar to the ones reported in Ref. 16. However, the values of the relaxation rates are too small to be ascribed to V^{4+} sites in $VOMoO_4$. The comparison of $(1/T_2)^2$ with the second moment derived for the ^{51}V dipole-dipole interaction shows that this signal must be due to a few percent of ^{51}V nuclei, possibly belonging to V^{5+} impurities.

III. ANALYSIS OF THE DATA AND DISCUSSION

A. Electronic structure and superexchange couplings

The superexchange couplings J_1 and J_2 were estimated both theoretically, starting from electronic structure calculations, and experimentally from the temperature dependence of the susceptibility. The electronic structure of $VOMoO_4$ was calculated by using density functional theory (DFT) in the local density approximation (LDA). The tight-binding linear muffin-tin orbital method[18] (LMTO47 Stuttgart code) was adopted together with the exchange-correlation potential of Perdew and Zunger[19] while the lattice parameters were taken from Ref. 10.

In Fig. 10 the electronic structure of $VOMoO_4$ and the corresponding density of states (DOS), derived with the linear tetrahedron method, are shown. The DOS was checked to have already converged with a mesh of about 858 irreducible *k* points. One can notice that only two relatively narrow bands, well separated from all the others, cross the Fermi level (ϵ_F), which was set to zero energy. The density of states shows a pronounced feature around ϵ_F, i.e., in correspondence with these two bands. This feature is more evident in the lower part of Fig. 10 where these two bands and the DOS in the energy window $(-0.8,0.4)$ eV are reported. In order to minimize the linearization error in this energy window, we placed the linearization energies close to the Fermi level. The eigenvectors of the two conduction bands have mainly V d_{xy} character, mixed with some O_2 $p_{x/y}$ and, in the case of the lower-energy band, with some Mo d_{xy} character. At the Γ point the two conduction bands are, respectively, the bonding (lower energy) and antibonding (higher energy) V d_{xy} bands.

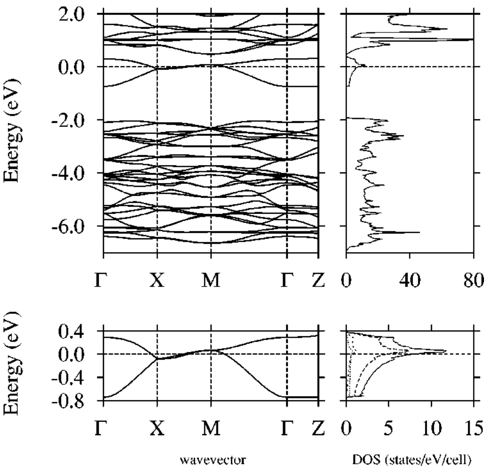

FIG. 10. (Top) Band structure (left) and density of states (right) of $VOMoO_4$. The Fermi level is set at zero energy. The symmetry points are $\Gamma=(0,0,0)$, $X=(\pi/a,0,0)$, $M=(\pi/a,\pi/a,0)$, and $Z=(0,0,\pi/c)$. (Bottom) Band structure of $VOMoO_4$ close to the Fermi level. On the right side the total DOS (solid line) is shown. The V *d* projected DOS (dashed line) and the O *p* and Mo *d* projected DOS (dash-dotted and dotted lines) are also shown.

The LDA bands can be understood from a few-band tight-binding model, as shown in the Appendix, and the dispersion curve of the two conduction bands can be written in terms of the nearest-neighbor (NN) (t_1) and next-nearest-neighbor (NNN) (t_2) hoppings within the (001) plane and of the hopping between adjacent planes ($t_\perp$):

$$\epsilon(\mathbf{k})=\epsilon_0+2t_2[\cos(k_xa)+\cos(k_ya)] + 4t_1[\cos(k_xa/2)\cos(k_ya/2)]+2t_\perp\cos(k_zc). \quad (5)$$

Their values can be estimated from a least-squares fitting of the calculated band structure. The results are shown in Table I. The NN hopping t_1 and the NNN hopping t_2 have two contributions of opposite sign. The first one originates from the hopping between V and NN O orbitals while the second one from hoppings involving V and NN O and Mo orbitals.

TABLE I. Hopping integrals (in meV) for $VOMoO_4$. The Coulomb repulsion is in eV and the exchange coupling constants are in K.

	t_1	t_2	$t_\perp$	U	J_1	J_2	$J_\perp$	J_1/J_2
Lower band	-110	-52	-1	5	110	22	$<10^{-2}$	4.5
Higher band	$+135$	-42	-2	5	154	16	$<10^{-2}$	10

The sign is different because while the energy of O *p* orbitals lies below the Fermi level the one of Mo *d* orbitals is above (see the Appendix). The contribution coming from Mo depends mainly on the energy of Mo d_{xy} effective orbital, whose energy is affected by the hopping with V d_{z^2} and, therefore, depends on V-Mo distance. Thus, the closer V is to Mo, the higher is the energy of Mo d_{xy} and the smaller the contribution of Mo to t_2 and t_1. In addition, the hopping between O *p* and Mo d_{xy} states tends to enhance the ratio t_1/t_2 (see the Appendix).

The hopping integrals can now be used to estimate the exchange couplings among V^{4+} spins. $VOMoO_4$ is a half-filled band Hubbard insulator and, in the limit of strong Coulomb repulsion, the exchange couplings can be expressed as $J_i = 4t_i^2/(U - V_i)$. Here t_i are the NN and NNN hoppings, U the on-site Coulomb repulsion, and V_i the intersite Coulomb repulsion, which is supposed to be much smaller than U. It was shown[20] that typical values of U for the vanadates are $U \sim 4-5$ eV. So by taking $U \sim 5$ eV and neglecting V_i the coupling values shown in Table I were derived.

First one notices that $J_\perp$ is at least four orders of magnitude smaller than the in-plane coupling constants, pointing out that $VOMoO_4$ is a 2D system and not a one-dimensional one as claimed by Shiozaki and co-workers.[11,12] Second, it should be observed that the value of $J_1 + J_2$ ranges between 132 and 170 K, in good agreement with the value $\Theta = J_1 + J_2 \simeq 155$ K derived experimentally for the Curie-Weiss temperature. On the other hand, for both bands we find $J_1 > J_2$, with J_1/J_2 around 4.5 for the lower-energy band and 10 for the higher-energy band. This result, however, seems in contrast with the experimental findings. In fact, the temperature dependence of the susceptibility and in particular the ratio between Θ and the temperature of the maximum in the susceptibility are very similar to the ones of Li_2VOSiO_4, pointing out that also, in $VOMoO_4$, $J_2/J_1 \simeq 1$. The similarity becomes evident once χ is plotted as a function of T/Θ (see Fig. 11). It is interesting to observe that an analogous discrepancy between the ratio J_2/J_1 derived experimentally and the one estimated from electronic structure calculation was found by Rosner *et al.*[21] for Li_2VOSiO_4. Also in that case the estimate of $J_1 + J_2$ was in good agreement with the experimental one, while the value of J_2 was found to be about a factor of 10 larger than J_1, the opposite of what happens for $VOMoO_4$. To assure that the estimate of J_2/J_1 was not influenced by the method adopted for calculating the band structure, the coupling constants were calculated also for Li_2VOSiO_4 and a ratio $J_2/J_1 \simeq 10$ was found, in good agreement with the results of Rosner *et al.*[21] The big difference in the ratio calculated for Li_2VOSiO_4 and $VOMoO_4$ cannot be associated with a difference in the V-O distances, which are quite similar in both compounds, or with the small rotation of the basis of the VO_5 pyramid. This difference should rather be ascribed to the role of Mo d_{xy} orbitals in $VOMoO_4$ and of Li *s* orbitals in Li_2VOSiO_4. As already mentioned the hopping between O *p*–Mo d_{xy} tends to enhance the ratio J_1/J_2. On the other hand, in Li_2VOSiO_4 the hopping between O *p* and NN Li *s* orbitals gives a contribution to t_1 only, which has a sign opposite to the one due to the V *d*–O *p* hopping. Hence the hopping through Li *s* orbitals reduces t_1 and the ratio J_1/J_2.

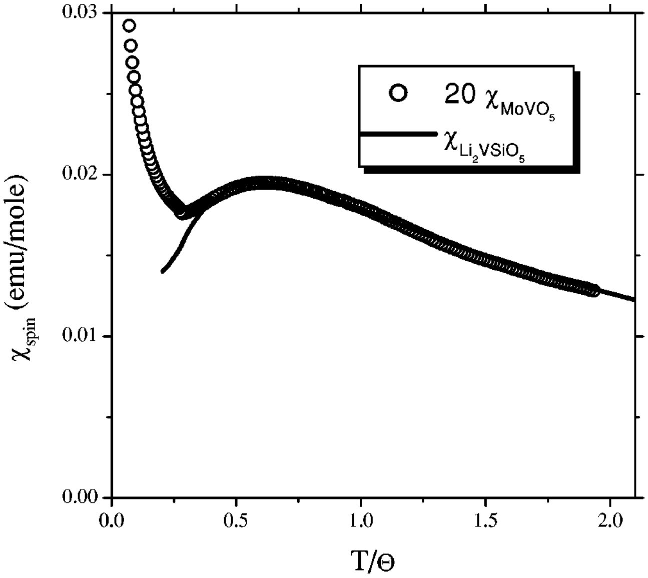

FIG. 11. Spin susceptibility of Li_2VOSiO_4 and $VOMoO_4$ as a function of T/Θ, with $\Theta = 8.7$ K and 155 K, respectively. The amplitude of the susceptibility of $VOMoO_4$ has been rescaled by a factor slightly larger than the ratio between the Curie-Weiss temperatures, indicating a slightly lower purity of the $VOMoO_4$ sample with respect to Li_2VOSiO_4.

Therefore, the observed discrepancies between the experimental and calculated values of J_2/J_1 cannot originate from the method adopted to calculate the band structure but must have another origin. They should rather be associated with the simplified expression used to derive the superexchange couplings, where just the on-site repulsion U was considered.

B. ^{95}Mo relaxation rates and EPR linewidth

As shown in the previous section ^{95}Mo echo decay, which probes the very-low-frequency dynamics, is characterized by two regimes: a high-temperature one where $1/T_2 = \Delta\omega'^2 \tau_c$ decreases on cooling and a low-temperature one where $1/T_2$ increases on approaching T_c from above. This means that the correlation time τ_c which describes the dynamics decreases on cooling from room temperature down to $T \simeq 100$ K. Which could be the origin of these dynamics? One possibility is that ^{95}Mo echo decay above 100 K is driven by the relaxation of unlike spins, namely, taking into account the natural abundance and the magnitude of the nuclear magnetic moments present in $VOMoO_4$, of ^{51}V spins. Then, $\tau_c \equiv T_1$ of ^{51}V and $\Delta\omega'$ corresponds to the nuclear dipole coupling between ^{95}Mo and ^{51}V nuclei which, from lattice sums, turns out $\Delta\omega' \simeq 1510$ s^{-1}. Now one can directly estimate ^{51}V $1/T_1$ from ^{95}Mo $1/T_2$ experimental data (see Fig. 12)[17,22].

One observes ^{51}V $1/T_1$ increasing exponentially on decreasing temperature, as one would expect for a correlated 2DQHAF.[23] In fact, the nuclear spin-lattice relaxation rate can be written as

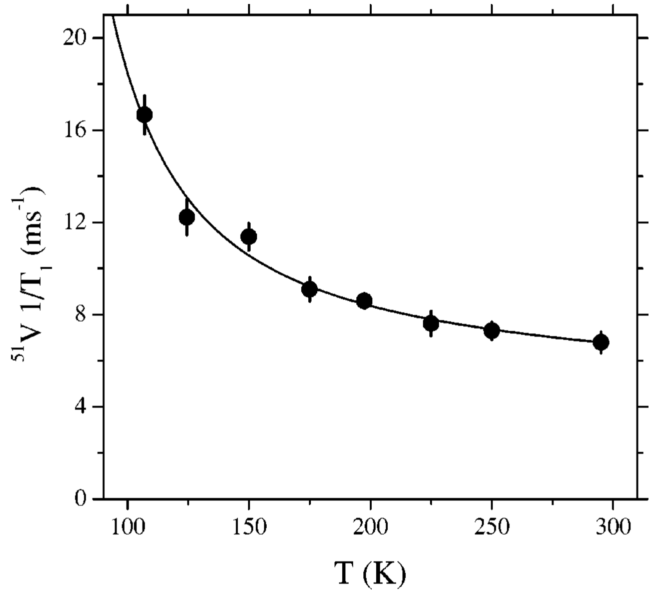

FIG. 12. Temperature dependence of ^{51}V NMR $1/T_1$ as estimated from the temperature dependence of ^{95}Mo $1/T_2$ shown in Fig. 9 (see Sec. III B). The line is a guide to the eye.

$$\frac{1}{T_1}=\frac{\gamma^2}{2N}\sum_{\vec{q}}|A(\vec{q})|^2_{\perp}S_{\alpha\alpha}(\vec{q},\omega_L),\qquad \alpha=x,y, \tag{6}$$

with $|A(\vec{q})|^2_{\perp}$ the form factor, which gives the hyperfine coupling of the nuclei with the spin excitations at wave vector $\vec{q}$, and $S_{\alpha\alpha}(\vec{q},\omega_L)$ the component of dynamical structure factor at nuclear Larmor frequency. If scaling arguments apply, one can express $S_{\alpha\alpha}(\vec{q},\omega_L)$ in terms of the in-plane correlation length and, provided that $VOMoO_4$ is in the renormalized classical regime and ^{51}V hyperfine coupling is mainly on site, one finds[23]

$$\frac{1}{T_1}(T)\propto\xi(T)$$
$$\simeq 0.49\exp(2\pi\rho_s/T)\left[1-\frac{1}{2}\left(\frac{T}{2\pi\rho_s}\right)\right], \tag{7}$$

with ρ_s the spin stiffness. If ^{51}V $1/T_1$ data are fitted with this simple expression, a poor fitting is obtained. The point is that most of the data obtained for ^{51}V $1/T_1$ lie in a temperature range where $T\geqslant J_1+J_2\simeq 155$ K and scaling arguments can no longer be applied. A more accurate quantitative analysis can be performed for $T\gg J_1+J_2$, where V^{4+} spins are uncorrelated. In this temperature limit one can write[24]

$$\frac{1}{T_1}=\frac{\gamma^2}{2}\frac{S(S+1)}{3}A^2_{\perp}\frac{\sqrt{2\pi}}{\omega_E}, \tag{8}$$

with $A_{\perp}$ ^{51}V hyperfine coupling constants and $\omega_E=\sqrt{J_1^2+J_2^2}(k_B/\hbar)\sqrt{2zS(S+1)/3}$ the Heisenberg exchange frequency, where $z=4$ is the number of V^{4+} coupled through J_1 or through J_2, to a reference V^{4+} ion. If one takes $1/T_1\simeq 6\ \mathrm{ms}^{-1}$ for $T\gg J_1+J_2$ (see Fig. 12), one derives $A_{\perp}\simeq 80$ kG. This is a typical value for V^{4+} hyperfine coupling,[25] supporting the assumption that vanadium nuclear spin-lattice relaxation is driving ^{95}Mo echo decay.

The increase in ^{95}Mo $1/T_2$ on approaching T_c must have a different origin since ^{51}V $1/T_1$ is expected to continue increasing on cooling and finally diverge at the transition temperature. The change of behavior around 100 K could be ascribed to the onset of a very-low-frequency dynamics, which is possibly associated with the motions of domain walls separating collinear I and II domains, as recently observed in Li_2VOSiO_4.[26]

It is interesting to compare the temperature dependence of ^{51}V and ^{95}Mo nuclear spin-lattice relaxation rates (see Figs. 8 and 12). One observes that while the former increases on cooling, the latter decreases. One could then be tempted to associate ^{95}Mo relaxation to another mechanism, for example a quadrupolar one, where the relaxation is due to phonons.[14] However, the nuclear spin-lattice relaxation rate due to phonons turns out to be an order of magnitude smaller than the one derived experimentally if the recovery laws appropriate for a quadrupolar relaxation mechanism are used.[27] On the other hand, if one estimates the value expected for $1/T_1$ in the assumption of a relaxation mechanism driven by V^{4+} dynamics for $T\gg J_1+J_2$ [Eq. (8)], the calculated value turns out to be slightly larger than the experimental one. So it is possible that the in-plane spin correlation causes a decrease of ^{95}Mo $1/T_1$. This is what is expected if the ^{95}Mo form factor filters out, at least partially, the spin fluctuations at the critical wave vector. In fact the ^{95}Mo form factor $|A(\vec{q})|^2=\{2A[\cos(q_xa/2)+\cos(q_ya/2)]\}^2$ is peaked at $(q_x=0,q_y=0)$, zero at $(\pi/a,\pi/a)$, and reaches a reduced value at $(\pi/a,0)$ [or $(0,\pi/a)$], which corresponds to the critical wave vector of the envisaged collinear ground state. This situation is very similar to the one found in CFTD (copper formiate tetradeuterate), a nonfrustrated 2DQHAF.[28] In this system ^{1}H has a form factor similar to the one of ^{95}Mo in $VOMoO_4$ and $1/T_1$ was also observed first to decrease on cooling for $T\leqslant J$ and then to increase. An accurate calculation of the temperature dependence of ^{95}Mo $1/T_1$ in $VOMoO_4$ goes beyond the aim of this work, since it would require precise knowledge of the temperature dependence of the hyperfine coupling constants between 220 K and T_c.

It is also instructive to compare ^{95}Mo $1/T_1$ with the EPR linewidth ΔH (see Fig. 3). The similarity in the temperature dependence of both quantities is striking. Although it is not straightforward to establish a relationship between these two quantities, the former probing the spectral density of the two-spin correlation function while the latter of the four-spins correlation function,[24] the physical origin of their behavior is the same. In fact, also the initial decrease of ΔH on cooling has to be associated with the loss of weight of the $q\rightarrow 0$ diffusive modes and to an increase in the spectral weight at $(\pi/a,0)$ [or $(0,\pi/a)$], which finally gives rise, in view of the slowing down of the critical fluctuations, to a peak at T_c.[29] As pointed out by Richards and Salamon (29) the transfer of spectral weight from $q\simeq 0$ to the critical wave vector causes also a modification in the angular dependence of ΔH, with first a decrease of $\Delta H_{ab}/\Delta H_c$ and then an increase, exactly as it was found for $VOMoO_4$ (see the inset to Fig. 3). For

$T \ll J_1 + J_2$, the EPR linewidth should scale with the in-plane correlation length, and if the same scaling laws derived for two-dimensional antiferromagnets[24] are used, one should find $\Delta H \propto \xi^3$. Then, by fitting the few experimental data in Fig. 3 for $T \leqslant 55$ K and assuming the temperature dependence of ξ given by Eq. (7) one derives a value for $2\pi\rho_s$ around 60 K, well below $J_1 + J_2$, as expected for a frustrated 2D antiferromagnet.[30]

C. Frustration-driven structural distortion

The analysis of NMR spectra points out that a local structural distortion around ^{95}Mo nuclei takes place at $T_{dist} \simeq 100$ K, yielding a sizable change of the magnetic hyperfine coupling (see Sec. II B). The occurrence of a structural distortion in $\mathrm{VOMoO_4}$ is a natural consequence of the frustration which, in the absence of a spin-lattice interaction, for $J_2/J_1 \simeq 1$ would lead to a double degenerate ground state down to a temperature where an Ising transition to one of the two ground states occurs.[31] The effect of the lattice is to relieve the degeneracy among the two ground states, so that the frustrated system always collapses in one of the two states. This is somewhat analogous to the Jahn-Teller distortion which relieves the degeneracy among the electronic levels split by the crystal field and for this reason some authors have called this distortion the ‘‘spin-Teller’’ distortion.[3,32] Recently, evidence for such a distortion in a three-dimensional pyrochlore antiferromagnet was presented.[33] On the other hand, some connection with the spin-Peierls distortion is also present. In fact, quite recently Becca and Mila[34] have shown that for a 2D J_1-J_2 system the magnetoelastic coupling would induce a distortion which, depending on the value of J_2/J_1 and on their dependence on the lattice parameters, could break either just the rotational invariance or, as for a standard spin-Peierls transition, also the translational invariance. Recent NMR measurements suggest that the breakdown of the rotational invariance takes place in $\mathrm{Li_2VOSiO_4}$.[35] In $\mathrm{VOMoO_4}$, however, the situation is somewhat more complicated than the one described by Becca and Mila[34] since J_1 and J_2 show a subtle dependence on Mo position and, therefore, cannot be expressed in a simple form in terms of the V-V distance.

Now, based on simple order-of-magnitude estimates one can show that the origin of the lattice distortion in $\mathrm{Li_2VOSiO_4}$ and $\mathrm{VOMoO_4}$ is the same. In fact, if one takes the ratio between the temperature at which the distortion sets in and $J_1 + J_2$, one finds $T_{dist}/(J_1 + J_2) = 0.5 \pm 0.07$ for $\mathrm{Li_2VOSiO_4}$ and a close value, 0.64 ± 0.07, for $\mathrm{VOMoO_4}$. This similarity can be understood by considering the expansion of the elastic and magnetic energies to lowest order in the displacements

$$E = \sum_{i,j,\alpha} (\partial J_{ij}/\partial x_\alpha)(\vec{S}_i \cdot \vec{S}_j) x_\alpha + \sum_{\alpha,\beta} k_{\alpha\beta} x_\alpha x_\beta /2, \qquad (9)$$

with $x_{\alpha,\beta}$ the coordinates of the magnetic ions coupled by an elastic constant $k_{\alpha,\beta}$. Since the reduction of magnetic energy is linear in x_α and the elastic one is quadratic, a minimum of magnetoelastic energy can be achieved for a small displacement x_{eq} of the coordinates. Now, if one considers just J_1 and J_2, couplings, the order of magnitude of the energy gain induced by the displacement turns out to be $E_{x_{eq}} \simeq -C[\partial(J_1 + J_2)/\partial x_\alpha]^2_{x_{eq}}/k_{x_{eq}}$, with C a constant which depends on the crystal structure. Then, if one considers that the similarities in $\mathrm{Li_2VOSiO_4}$ and $\mathrm{VOMoO_4}$ structure yield roughly similar elastic constants and power-law dependence of J_i on x_α, it is likely that $k_B T_{dist} \simeq E_{x_{eq}} \propto (J_1 + J_2)$, as experimentally found.

It is remarkable to observe that while a clear signature of such a distortion is present in the NMR spectra, no modification in $\mathrm{V^{4+}}$ $\tilde{g}$ tensor is detected down to T_c. On the other hand, below 100 K a decrease in the intensity of the EPR signal, much faster than the decrease of the macroscopic magnetization, is observed (see Figs. 3 and 4). This effect is not associated with a saturation or a broadening of the EPR signal but rather indicates that there are some ions that are becoming EPR silent. These ions cannot correspond to $\mathrm{V^{4+}}$, which in a pyramidal coordination such as the one in $\mathrm{VOMoO_4}$ should always give an EPR signal. However, if valence fluctuations take place, they could correspond to $\mathrm{Mo^{5+}}$ ions. In fact, due to selection rules, the signal of $\mathrm{Mo^{5+}}$ in a regular tetrahedral configuration is canceled out. The regular tetrahedral coordination is indeed supported by the small values of the ^{95}Mo quadrupolar frequency (see Sec. II B).

As a whole, the comparison of NMR and EPR spectra leads to the following possible scenario. The distortion induced by the frustration causes, thanks to the hybridization of Mo d orbitals in the band formation, a charge transfer from $\mathrm{V^{4+}}$ to $\mathrm{Mo^{6+}}$. As the distortion develops it induces a modification just in the NMR spectra of the adjacent nuclei, yielding a broadening of the NMR line (see Sec. II B) and the disappearance of the EPR signal of the adjacent $\mathrm{V^{4+}}$ ions. The $\mathrm{V^{4+}}$ ions far from the distortion continue to give rise to an EPR signal with unchanged g values, as experimentally observed. As the temperature is lowered, the size of the distorted domains progressively grows and the EPR signal diminshes. The formation of distorted and nondistorted domains would support also the modifications in ^{29}Si NMR spectra in $\mathrm{Li_2VOSiO_4}$.[5] In fact, in $\mathrm{Li_2VOSiO_4}$ as the temperature is lowered below T_{dist}, one observes the progressive decrease of a low-frequency peak (undistorted site) and the growth of a shifted high-frequency peak (distorted site) (see Ref. 5). Hence, at T_{dist} a diffusive transition sets in, yielding a progressive distortion of the whole lattice as the temperature decreases below 100 K.

It should be noticed that it is somewhat unusual that $\mathrm{Mo^{5+}}$ formation does not cause any Jahn-Teller effect. However, in this system the Jahn-Teller distortion could actually be hindered by the frustration-driven distortion. This can occur if the distortion yields an energy gain of the frustrated magnetic lattice larger than the shift of the t_{2g} ground state. The charge transfer could also induce a progressive crossover of $\mathrm{VOMoO_4}$ from a half-filled to a quarter-filled band configuration, as the one of $\mathrm{NaV_2O_5}$,[36] as the temperature decreases below 100 K and modifications in the transport properties should be observed. In fact, below 100 K a decrease in the energy barrier measured with resistivity is detected.[37]

IV. CONCLUSIONS

In conclusion, it was shown that $VOMoO_4$ is a prototype of a 2DFQHAF on a square lattice with $J_1 \simeq J_2$, such as Li_2VOSiO_4. The exchange couplings in $VOMoO_4$ are much larger than the ones of Li_2VOSiO_4 and a value $J_1+J_2 \simeq 155$ K was derived, in good agreement with the one estimated from electronic structure calculations. In $VOMoO_4$ a lattice distortion takes place at $T_{dist} \simeq 100$ K. As the temperature is lowered below T_{dist} a progressive growth of the domains with lattice distortion occurs. From the comparison with Li_2VOSiO_4 one finds that in these 2DFQHAF T_{dist} roughly scales with J_1+J_2, supporting the assumption that the distortion is driven by the magnetic frustration. Finally, in $VOMoO_4$, novel phenomena, not observed in Li_2VOSiO_4, occur below T_{dist} and are tentatively associated with a charge transfer from V to Mo.

ACKNOWLEDGMENTS

The authors would like to thank F. Becca and A. Rigamonti for useful discussions. The research activity in Pavia was supported by INFM Project No. PA-MALODI.

APPENDIX: TIGHT-BINDING MODEL

The simplest model which can be used to describe the bands derived in the framework of the LDA includes 12 orbitals. The d_{xy} of V_1 and V_2 (energy ϵ_d), where V_1 is the atom at $(1/4,1/4,z_V)$ and V_2 is the atom at $(-1/4,-1/4,-z_V)$; the four O p_x orbitals (energy ϵ_p) centered in $(\pm(1/4-\delta_1),\mp\delta_2,\mp z_O)$ and $(\pm(1/4+\delta_1,\mp 1/2\pm\delta_2,\mp z_O)$; the four O p_y orbitals (energy ϵ_p) centered in $(\mp\delta_1,\pm(1/4+\delta_2),\mp z_O)$ and $((\mp 1/2\pm\delta_1),\pm(1/4-\delta_2),\mp z_O)$; and the two Mo centered in $(1/4,-1/4,1/2)$ and $(-1/4,1/4,1/2)$ (energy ϵ_m). Within this model the following hopping integrals are considered: the hoppings between V d and O p states (t_{pd}), the hopping between NN O p_x and O p_y orbitals (t_{oo}), and the hopping between Mo d_{xy} and its NN O p_x and O p_y orbitals (t_{mo}). Starting from this band model the dispersion curve of the two conduction bands can be obtained by downfolding all the O and V states.[38] Setting $\delta_1=\delta_2=0$ and neglecting $t_\perp$ one has

$$\epsilon=\epsilon_d+8\frac{t_{pd}^2}{\epsilon-\epsilon_p}+4\frac{t_{pd}^2}{\epsilon-\epsilon_p}\frac{b}{1-b}[\cos^2(k_x/2)+\cos^2(k_y/2)] \pm 8\frac{t_{pd}}{\epsilon-\epsilon_p}\frac{a}{1-b}\cos(k_x/2)\cos(k_y/2), \tag{A1}$$

with

$$b=16\frac{t_{oo}^2}{(\epsilon-\epsilon_p)^2}+4\frac{t_{mo}^2}{(\epsilon-\epsilon_p)(\epsilon-\epsilon_m)}\left(1+4\frac{t_{oo}}{(\epsilon-\epsilon_p)}\right)^2$$

and

$$a=\frac{4t_{oo}}{(\epsilon-\epsilon_p)}+4\frac{t_{mo}^2}{(\epsilon-\epsilon_p)(\epsilon-\epsilon_m)}\left(1+4\frac{t_{oo}}{(\epsilon-\epsilon_p)}\right).$$

Then one has that the in-plane NN and NNN hoppings are

$$t_1=2\frac{t}{\epsilon-\epsilon_p}\frac{a}{1-b}$$

and

$$t_2=2\frac{t^2}{\epsilon-\epsilon_p}\frac{b}{1-b},$$

so that $J_2/J_1 \simeq (t_2/t_1)^2=b^2/a^2$.

---

*Electronic address: carretta@fisicavolta.unipv.it

[1] See, for example, E. Dagotto, T. Hotta, and A. Moreo, Phys. Rep. **344**, 1 (2001).
[2] M. Hase, I. Terasaki, and K. Uchinokura, Phys. Rev. Lett. **70**, 3651 (1993).
[3] Y. Yamashita and K. Ueda, Phys. Rev. Lett. **85**, 4960 (2000).
[4] See L. Capriotti, Int. J. Mod. Phys. B **14**, 3386 (2000) and references therein.
[5] R. Melzi, P. Carretta, A. Lascialfari, M. Mambrini, M. Troyer, P. Millet, and F. Mila, Phys. Rev. Lett. **85**, 1318 (2000).
[6] R. Melzi, S. Aldrovandi, F. Tedoldi, P. Carretta, P. Millet, and F. Mila, Phys. Rev. B **64**, 024409 (2001).
[7] H.J. Schulz and T.A.L. Ziman, Europhys. Lett. **18**, 355 (1992); V.N. Kotov, M.E. Zhitomirsky, and O.P. Sushkov, Phys. Rev. B **63**, 064412 (2001).
[8] P. Chandra and B. Doucot, Phys. Rev. B **38**, 9335 (1988).
[9] P. Millet and C. Satto, Mater. Res. Bull. **33**, 1339 (1998).
[10] H.A. Eick and L. Kihlborg, Acta Chem. Scand. **20**, 722 (1966).
[11] I. Shiozaki, J. Phys.: Condens. Matter **10**, 9813 (1998); I. Shiozaki, M. Ohashi, M. Kayano, and S. Katayama, Physica B **284-288**, 1621 (2000); K. Narushima and I. Shiozaki, Solid State Commun. **101**, 99 (1996).
[12] I. Shiozaki, J. Magn. Magn. Mater. **177-181**, 261 (1998).
[13] M.C. Mozzati, C.B. Azzoni, and P. Carretta (unpublished).
[14] A. Abragam, in *Principles of Nuclear Magnetism* (Oxford University Press, New York, 1961).
[15] K.D. Sen and P.T. Narasimhan, Phys. Rev. B **15**, 95 (1977).
[16] S. Takata, S. Wada, and I. Shiozaki, J. Phys. Soc. Jpn. **70**, 1124 (2001).
[17] R.E. Walstedt and S.-W. Cheong, Phys. Rev. B **51**, 3163 (1995).
[18] O.K. Andersen and O. Jepsen, Phys. Rev. Lett. **53**, 2571 (1984).
[19] J.P. Perdew and A. Zunger, Phys. Rev. B **23**, 5048 (1981).
[20] A.T. Mizokawa and A. Fujimori, Phys. Rev. B **48**, 14 150 (1993); J. Zaanen and G.A. Sawatzky, J. Solid State Chem. **88**, 8 (1990); K. Held, Phys. Rev. Lett. **86**, 5345 (2001).
[21] H. Rosner, R.R.P. Singh, W.H. Zheng, J. Oitmaa, S.-L. Drechsler, and W.E. Pickett, Phys. Rev. Lett. **88**, 186405 (2002).
[22] C.H. Recchia, J.A. Martindale, C.H. Pennington, W.L. Hults, and J.L. Smith, Phys. Rev. Lett. **78**, 3543 (1997).
[23] P. Carretta, A. Rigamonti, and R. Sala, Phys. Rev. B **55**, 3734 (1997).

[24] H. Benner and J.P. Boucher, in *Magnetic Properties of Layered Transition Metal Compounds*, edited by L.J. De Jongh (Kluwer Academic, Norwell, MA, 1990), p. 323.

[25] A.V. Mahajan, R. Sala, E. Lee, F. Borsa, S. Kondo, and D.C. Johnston, Phys. Rev. B **57**, 8890 (1998).

[26] P. Carretta, R. Melzi, N. Papinutto, and P. Millet, Phys. Rev. Lett. **88**, 047601 (2002).

[27] M.I. Gordon and M.J.R. Hoch, J. Phys. C **11**, 783 (1978).

[28] P. Carretta, T. Ciabattoni, A. Cuccoli, E. Mognaschi, A. Rigamonti, V. Tognetti, and P. Verrucchi, Phys. Rev. Lett. **84**, 366 (2000).

[29] P.M. Richards and M.B. Salamon, Phys. Rev. B **9**, 32 (1974).

[30] H.J. Schulz, T.A.L. Ziman, and D. Poilblanc, J. Phys. I **6**, 675 (1996).

[31] P. Chandra, P. Coleman, and A.I. Larkin, Phys. Rev. Lett. **64**, 88 (1990).

[32] O. Tchernyshyov, R. Moessner, and S.L. Sondhi, Phys. Rev. Lett. **88**, 067203 (2002).

[33] A. Keren and J.S. Gardner, Phys. Rev. Lett. **87**, 177201 (2001).

[34] F. Becca and F. Mila, Phys. Rev. Lett. **89**, 037204 (2002).

[35] N. Papinutto and P. Carretta (unpublished).

[36] T. Ohama, H. Yasuoka, M. Isobe, and Y. Ueda, Phys. Rev. B **59**, 3299 (1999); Y. Fagot-Revurat, M. Mehring, and R.K. Kremer, Phys. Rev. Lett. **84**, 4176 (2000).

[37] I. Shiozaki, M. Ohashi, and H. Kadowaki, J. Phys. Soc. Jpn. **69**, 3873 (2000).

[38] O.K. Andersen, A.I. Liechtestein, O. Jepsen, and F. Paulsen, J. Phys. Chem. Solids **56**, 1573 (1995).